

Spectroscopy with multiple field configurations

A. Krasnitz

Physics Department, Indiana University, Swain Hall-West 117, Bloomington, Indiana 47405

(Received 19 December 1990)

The effect of field configuration copying on both fermion and fermion-antifermion pair correlation functions is studied in detail in a simple quantum-mechanical model. It is found that, with very few exceptions, the copying procedure results in a large correction to the corresponding effective masses. In particular, this correction leads to an oscillatory behavior of the effective masses, similar to that observed for mesons in recent lattice QCD calculations. It is argued that the copying technique is unlikely to be useful as a spectroscopic tool.

I. INTRODUCTION

Over the last decade the following technique has been frequently applied in lattice calculations: time size of a lattice is artificially enlarged by copying gauge configurations several times in the time direction.¹⁻⁵ These enlarged lattices are then used to calculate hadronic correlation functions. By using this trick one could hope to obtain a wider separation between a source and a sink corresponding to matter fields. In doing so, however, one should be aware of a distorting effect this procedure might have on correlation functions, and, consequently, on the measured particle spectrum. Indeed, an unexpected behavior of the pion propagator found in the recent high-statistics QCD simulation⁵ is believed to be due to such an effect. Similar indications can be found in non-relativistic QCD calculations.⁴ While the analysis of this phenomenon in QCD itself appears to be a difficult task, some useful information may be obtained from much less complicated models. In a recent Rapid Communication⁶ we considered a simple quantum-mechanical example and showed that an oscillatory behavior of the fermion effective mass may arise from copying the background Bose field configuration. In the present work the study of the configuration copying in this model is carried out in more detail. In Sec. II the fermion propagator is dealt with in all the copies. We also consider the effect of the nonzero bare fermion mass. In Sec. III we study an extension of

the model with two fermionic degrees of freedom. This allows us to observe the configuration copying effects in the fermion-antifermion bound-state ("meson") correlation function. We then discuss the meaning of our results and their implications for other models (Sec. IV). The Appendix contains the description of our numerical method.

II. ONE-FERMION CASE

Let the problem be described by the Hamiltonian

$$H = \omega a^\dagger a - [\lambda(a + a^\dagger) + \mu]c^\dagger c, \quad (1)$$

where a and c correspond to boson and fermion degrees of freedom, respectively: $[a, a^\dagger] = \{c, c^\dagger\} = 1$. This is in fact a problem of a particle moving in harmonic-oscillator potential with its spin $\frac{1}{2}$ coupled to a magnetic field. The latter is a linear function of the oscillator coordinate. The oscillator frequency ω is assumed to be positive, and so is the fermion bare mass μ . In order to simplify the notation, we shall assume all the dimensionful quantities to be given in temperature units. One can verify the following expressions for the partition function

$$Z \equiv \text{Tre}^{-H} = \frac{1 + e^{\lambda^2/\omega + \mu}}{1 - e^{-\omega}} \quad (2)$$

and for the fermion correlation function

$$C_1(\tau) = \text{Tr}(c^\dagger e^{-\tau H} c e^{-(1-\tau)H}) \\ = \exp \left[\frac{\lambda^2}{\omega^2} \left(\omega(1-\tau) + e^{-\omega(1-\tau)} - 1 + \frac{(1 - e^{-\omega(1-\tau)})^2}{1 - e^{-\omega}} e^{-\omega\tau} \right) + \mu(1-\tau) \right] \quad (3)$$

(the meaning of the subscript 1 will be clarified in the following). The fermion effective mass is customarily defined as a logarithmic derivative of $C_1(\tau)$:

$$m_{\text{eff}} \equiv -\frac{d}{d\tau} \ln C_1(\tau) = M \left(1 + \frac{\sinh[\omega(\frac{1}{2} - \tau)]}{\sinh(\omega/2)} \right) + \mu, \quad (4)$$

where

$$M \equiv \frac{\lambda^2}{\omega}. \quad (5)$$

The quantity $M + \mu$ is an energy gap associated with the fermion. It clearly represents the energy penalty for the spin pointing against the field direction. The time-dependent term in Eq. (4) is a finite-temperature correction apparently coming from the excited states of both the oscillator and the spin. In the low-temperature regime ($\omega \gg 1$) this contribution is negligible if both $1 - \tau$ and τ are large compared to ω^{-1} , i.e., everywhere in the interval $0 \leq \tau \leq 1$ except close vicinities of its edges.

Our purpose is to study the time evolution of the fermion (c, c^\dagger) interacting with the replicated Bose field (a, a^\dagger). This is usually done in three steps. First we represent the partition function Z as a functional integral over the anticommuting and the c -number fields corre-

sponding to the fermion and the boson, respectively. The fermions are then integrated out, resulting in an effective interaction between the c -number fields. Finally, the fermion propagator is averaged over the Bose background configurations. In our previous work on the subject⁶ we followed these three steps explicitly. Here we give a simple alternative derivation which is most easily generalized for more than one fermionic degree of freedom. Taking trace over the fermionic states in the partition function we see that

$$\text{Tr} e^{-H} = \text{Tr}_B \{ \exp(-\omega a^\dagger a) + \exp[-\omega a^\dagger a + \lambda(a + a^\dagger) + \mu] \}, \quad (6)$$

where the subscript B denotes a trace over the bosonic states only. Using the resolution of unity in terms of eigenstates of a we then obtain the following path-integral representation for the partition function:^{7,8}

$$Z = \left(\frac{1}{2\pi} \right)^n \int \prod_{m=0}^{n-1} dz_m d\bar{z}_m \left[1 + \exp \left(\mu + ng + f \sum_{j=0}^{n-1} (\bar{z}_j + z_j) \right) \right] e^{S_B}. \quad (7)$$

with the definitions $g \equiv (\frac{\lambda}{\omega})^2 (\epsilon\omega + e^{-\epsilon\omega} - 1)$, $f \equiv \frac{\lambda}{\omega} (1 - e^{-\epsilon\omega})$, and $\epsilon \equiv n^{-1}$. Here the unit imaginary-time interval is split into n subintervals with pairs of complex c -number variables z, \bar{z} corresponding to the intermediate points. In order for Eq. (7) to reproduce Eq. (2) periodic boundary conditions in time are to be assumed for z, \bar{z} . The pure bosonic action reads

$$S_B = \sum_{m=0}^{n-1} (e^{-\epsilon\omega} \bar{z}_{m+1} z_m - \bar{z}_m z_m). \quad (8)$$

The prefactor of e^{S_B} in Eq. (7) is generated by the

fermions. Note that ϵ is not assumed to be small, i.e., Z as given by Eq. (7) is independent of n and coincides with Eq. (2). The same should be true for the fermion correlation function, but, as will be shown in the following, using repeated field configurations leads to deviations persisting in both the continuum ($\epsilon \rightarrow 0$) and the zero-temperature ($\omega, \mu, M \rightarrow \infty$) limits.

The path-integral form of the fermion correlation function $C_1(\tau)$ is derived in precisely the same way, with $\text{Tr} e^{-H}$ replaced by $\text{Tr}(c^\dagger e^{-\tau H} c e^{-(1-\tau)H})$. Assuming for the definiteness $0 < \tau = \epsilon l < 1$ we have

$$C_1(\tau) = e^{(1-\tau)\mu} \left(\frac{1}{2\pi} \right)^n \int \prod_{m=0}^{n-1} dz_m d\bar{z}_m \exp \left(g(n-l) + f \sum_{j=0}^{n-1} (\bar{z}_j + z_j) - f \sum_{j=1}^l (\bar{z}_j + z_{j-1}) + S_B \right). \quad (9)$$

Comparing Eq. (9) with Eq. (7) we find the expression for the fermion propagator in a given z field background:

$$\Pi_1(\tau, z, \bar{z}) = \frac{\exp \left(-\tau(\mu + ng) - f \sum_{j=1}^l (\bar{z}_j + z_{j-1}) \right)}{1 + \exp \left[- \left(\mu + ng + f \sum_{j=0}^{n-1} (\bar{z}_j + z_j) \right) \right]}. \quad (10)$$

We are now in a position to write down the fermion propagator in the repeated N times z field configuration. It is obtained from Eq. (10) if we replace n by nN while retaining the periodic boundary conditions with unit period on z fields. Representing the lattice time separation l as $kn + l(\text{mod } n)$ (k is an integer) we have

$$\Pi_N(t, z, \bar{z}) = \frac{\exp \left(-\tau(\mu + ng) - kf \sum_{j=0}^{n-1} (\bar{z}_j + z_j) - f \sum_{j=1}^{l(\text{mod } n)} (\bar{z}_j + z_{j-1}) \right)}{1 + \exp \left[-N \left(\mu + ng + f \sum_{j=0}^{n-1} (\bar{z}_j + z_j) \right) \right]}. \quad (11)$$

The corresponding correlation function $C_N(\tau)$ can now be obtained by averaging Π_N over the z field configurations with the weight as given by Eq. (7). In the $N = 1$ case the result Eq. (3) is recovered upon the integration over \bar{z} , z , and the dependence on the lattice spacing ϵ disappears. Once $C_1(\tau)$ is known, $C_N(\tau)$ for an arbitrary value of N may be found indirectly. To this end we notice that the averaging over different Fourier components of the z field can be performed independently and that Π_N differs from Π_1 only in its dependence on the zero-frequency component. Thus C_N/C_1 is just the ratio of one-dimensional integrals:

$$\frac{C_N(\tau)}{C_1(\tau - k)} = \frac{F_N(\tau)}{F_1(\tau - k)}, \tag{12}$$

where

$$F_N(\tau) \equiv \int du \frac{1 + e^{\mu + ng + 2bu}}{1 + e^{N(\mu + ng + 2bu)}} \times \exp\left((N - \tau)(\mu + ng + 2bu) - \frac{b}{\sqrt{M}}u^2\right) \tag{13}$$

with the definitions $u \equiv \frac{\sqrt{\omega}}{2n} \sum_{j=0}^{n-1} (\bar{z}_j + z_j)$ and $b \equiv \frac{nf}{\sqrt{\omega}}$. The ratio Eq. (12), as well as $C_N(\tau)$ itself is in general n (or ϵ) dependent. From now on we restrict the discussion to the continuum limit $\epsilon \rightarrow 0$. In the latter case g must be replaced by 0 and $b = \sqrt{M}$. As a consequence, the Gaussian factor in Eq. (13) becomes e^{-u^2} .

The correlation-function and the effective-mass corrections following from Eq. (12) will now be studied analytically for limiting values of M and μ . This study will be complemented by a numerical analysis for intermediate values of these parameters using the method described in the Appendix. Before doing so, a number of remarks should be made. First of all, we note that the oscillator frequency ω does not appear in the continuum limit of F_N . The configuration copying yields corrections to m_{eff} whose finite-temperature scale is M rather than ω [cf. Eq. (4)]. We can therefore fix ω with no loss of generality. Second, our analysis is equally valid for any $N > 1$. For the purpose of illustration we choose $\omega = 5.5$ and $N = 4$. Finally, it should be noted that we find a perfect agreement between the analytical and the numerical results wherever the comparison is possible.

Consider the massless ($\mu = 0$) fermion first. In the high-temperature ($M \ll 1$) limit the Gaussian is the most rapidly varying factor in the integrand of Eq. (13), and $F_N(\tau)$ can therefore be computed by the steepest-descent method, giving

$$\frac{F_N(\tau)}{F_1(\tau - k)} = \exp \left[M \left(\frac{N}{2} - \frac{1}{2} - k \right) \times \left(\frac{3}{2}N + \frac{1}{2} + k - 2\tau \right) \right]. \tag{14}$$

It follows that the corresponding correction to the fermion effective mass in this regime depends only on k , the integer part of τ :

$$\Delta m_{\text{eff}} = M(N - 1 - 2k). \tag{15}$$

This means that the shape of $m_{\text{eff}}(\tau)$ in every system copy is as given by Eq. (4) for $N = 1$ up to a constant. The size of this constant (a multiple of M) is precisely as needed to ensure the continuity of $m_{\text{eff}}(\tau)$ across a copy boundary. The high-temperature regime is illustrated by the $M = 0.01$ curve of Fig. 1. Note that Δm_{eff} is generally of order M . The only exception is vanishing Δm_{eff} in the $[(N + 1)/2]$ th copy for odd N .

A completely different behavior occurs in the low-temperature ($M \gg 1$) limit. If τ is deep inside the interval $[1, N]$, the integrand of Eq. (13) is non-negligible only for u of order $M^{-1/2}$. With the zero-frequency component of the z field driven to the close vicinity of 0, the fermion propagator [Eq. (11)] becomes a periodic function of the time separation, and so does $C_N(\tau)$. To make this argument more quantitative we note that this time the Gaussian in Eq. (11) is a slowly varying function and may be safely replaced by 1. Therefore

$$F_N(\tau) = \frac{\pi}{2N\sqrt{M}} \left[\csc \left(\pi \frac{\tau - N}{N} \right) + \csc \left(\pi \frac{\tau - N - 1}{N} \right) \right]. \tag{16}$$

This amounts to a negligible (of order M^{-1}) relative correction to the fermion effective mass. The major correction to $m_{\text{eff}}(\tau)$ comes only from $F_1(\tau - k)$, namely, in this case

$$\Delta m_{\text{eff}}(\tau) = 2M(\tau - k - 1). \tag{17}$$

Superposing this correction with $m_{\text{eff}}(\tau - k)$ as given by Eq. (4) we find that the fermion effective mass oscillates around zero. It is not difficult to show that the amplitude of these oscillations monotonically grows from 0 to M as the oscillator frequency ω varies from 0 to ∞ . If τ is within the first copy ($0 < \tau < 1$), F_N and F_1 are roughly equal. Indeed,

$$F_N(\tau) = F_1(\tau) + \int du \frac{e^{2(N-1)\sqrt{M}u} - 1}{1 + e^{2N\sqrt{M}u}} e^{2(1-\tau)\sqrt{M}u - u^2} = \sqrt{\pi} e^{M(1-\tau)^2} + \frac{\pi}{2N\sqrt{M}} \left[\csc \left(\pi \frac{\tau - N}{N} \right) - \csc \left(\pi \frac{\tau - 1}{N} \right) \right], \tag{18}$$

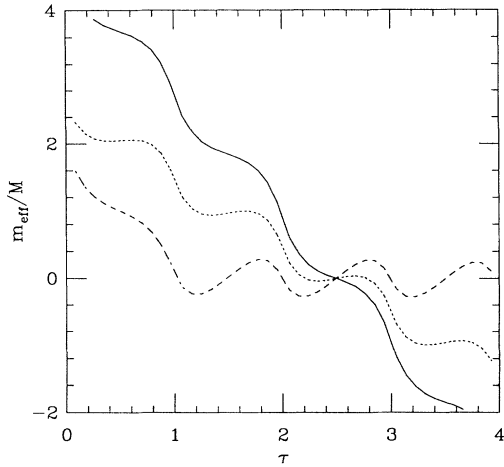


FIG. 1. Fermion effective mass curves at $\mu = 0$ for $M = 0.01$ (solid curve), 0.25 (dotted curve), and 100 (dashed curve).

and the correction to F_1 is exponentially small for large M . This in turn means that the fermion effective mass in the first copy is given by Eq. (4) to a good approximation. The $M = 100$ curve of Fig. 1 reflects the low-temperature behavior of the effective mass. The intermediate-temperature case is represented by the $M = 0.25$ curve of the same figure; it combines the k -dependent copy shift with a tendency towards oscillations.

Similar simple estimates apply to a more general case of a nonzero fermion bare mass. If the latter is small compared to the dynamically generated one (i.e., $\mu \ll M$), it will have very little effect on the correlation function. If, however, the opposite condition holds, the dynamics of the fermion is dominated by the bare mass term, the interaction being a small perturbation. Technically this means that we can replace the integrand of $F_N(\tau)$ by its approximate form in the vicinity of the Gaussian peak:

$$F_N(\tau) = F_1(\tau). \quad (19)$$

The corresponding correction to the effective mass is therefore

$$\Delta m_{\text{eff}} = -2kM. \quad (20)$$

This behavior is similar to the one we found in the massless high-temperature case, only this time the effective-

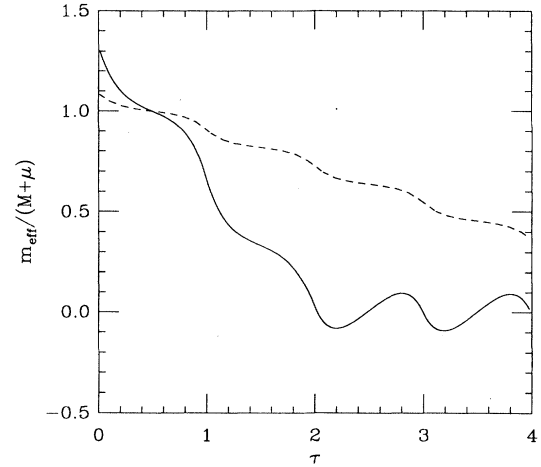


FIG. 2. Effective mass curves for massive fermions: $\mu = 200$ (solid curve) and 10^3 (dashed curve). In both cases $M = 100$.

mass correction vanishes in the first copy. As expected, the correction is small compared to the exact energy-gap value. A typical large- μ effective mass curve is shown in Fig. 2 ($\mu = 10^3$). Also shown is the m_{eff} curve for the moderately heavy ($\mu = 200$) fermion; note that the bare mass is sufficiently large to suppress the oscillations in the second, but not in the third and the fourth copies.

III. FERMION-ANTIFERMION PAIR CASE

Having in mind possible implications for lattice QCD, we would like to study time evolution of fermion-antifermion bound states rather than that of individual fermions. To this end we extend our simple model in order to accommodate such a state. The following discussion parallels that of the preceding section, and technical details will therefore be given less explicitly. Consider the Hamiltonian

$$H = \omega a^\dagger a + [\lambda(a + a^\dagger) + \mu](c_+^\dagger c_+ - c_-^\dagger c_-), \quad (21)$$

where the two fermionic degrees of freedom are denoted by c_\pm . The energy level structure of H is obvious. The ground state is annihilated by c_+ , c_-^\dagger , and $a + \frac{\lambda}{\omega}$. The particle-hole excitation (called meson in the following) is created by applying $c_+^\dagger c_-$ to the ground state and is separated from the latter by a gap 2μ . The corresponding correlation function is

$$\begin{aligned} C_1(\tau) &= \text{Tr}(c_-^\dagger c_+ e^{-\tau H} c_+^\dagger c_- e^{-(1-\tau)H}) \\ &= \exp \left[\frac{4\lambda^2}{\omega^2} \left(e^{-\omega(1-\tau)} - 1 + \frac{(1 - e^{-\omega(1-\tau)})^2}{1 - e^{-\omega}} e^{-\omega\tau} \right) + \mu(1 - 2\tau) \right] \end{aligned} \quad (22)$$

and the meson effective mass is given by

$$m_{\text{eff}} \equiv -\frac{d}{d\tau} \ln C_1(\tau) = 4M \frac{\sinh[\omega(\frac{1}{2} - \tau)]}{\sinh(\omega/2)} + 2\mu. \quad (23)$$

Again, as in the one-fermion case, $m_{\text{eff}}(\tau)$ at low temperatures approaches the meson energy gap if τ is far enough from both 0 and 1.

The derivation of $C_N(\tau)$ for the meson exactly follows the preceding section [Eqs. (9)–(13)]. As a result, we obtain in complete analogy with Eq. (12),

$$\frac{C_N(\tau)}{C_1(\tau - k)} = \frac{G_N(\tau)}{G_1(\tau - k)}, \quad (24)$$

where, in the continuum limit,

$$G_N(\tau) \equiv \int du \frac{1 + \cosh(2\sqrt{M}u)}{1 + \cosh(2N\sqrt{M}u)} \times e^{2\sqrt{M}(N-2\tau)u - (u - \mu/2\sqrt{M})^2}. \quad (25)$$

Again, the limiting cases are most easily understood. We begin with the $\mu = 0$ limit, where the meson energy gap should vanish. At high temperatures we obtain, by applying the steepest-descent approximation to G_N ,

$$\Delta m_{\text{eff}} = 4M(N - 1 - 2k) \quad (26)$$

in a close analogy with Eq. (15). This type of behavior is illustrated by the upper curve of Fig. 3. Note that only two copies out of four are shown because the mesonic $m_{\text{eff}}(\tau)$ is an odd function of $\tau - N/2$ for $\mu = 0$.

At low temperatures the Gaussian factor in Eq. (25) may be replaced by 1 for $\frac{1}{2} < \tau < N - \frac{1}{2}$. In this range of τ values we obtain, closely following Eq. (17),

$$\Delta m_{\text{eff}}(\tau) = 4M(2\tau - 2k - 1). \quad (27)$$

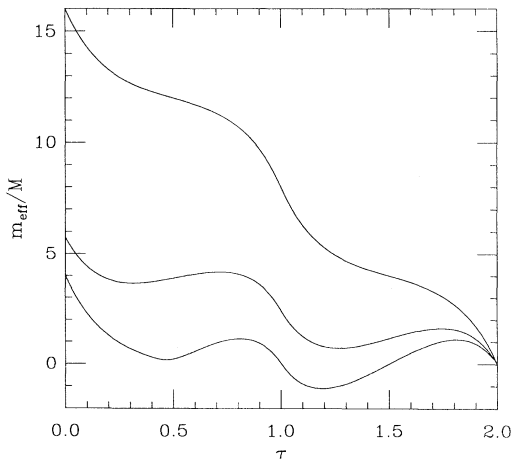


FIG. 3. Meson effective mass curves at $\mu = 0$ for $M = 0.00625$ (upper curve), 0.25 (medium curve), and 100 (lower curve).

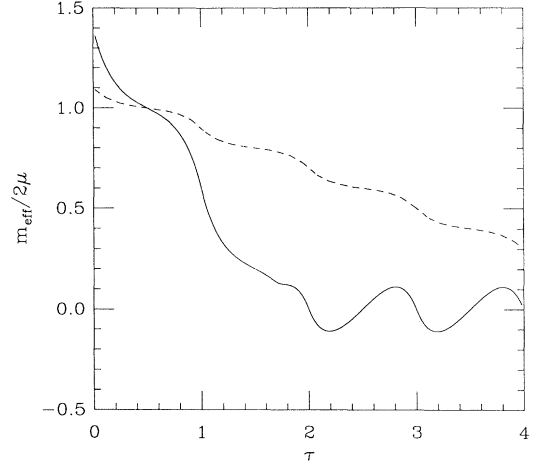


FIG. 4. Effective mass curves for mesons with nonzero fermion bare mass: $\mu = 500$ (solid curve) and 2×10^3 (dashed curve). In both cases $M = 100$.

This correction leads to an oscillatory behavior familiar from the one-fermion case. Note, however, that this time the oscillations set in already in the first copy. This is hardly surprising: one would expect a similar result even for an uncorrelated fermion-antifermion pair, as can be shown by superposing the fermionic low-temperature effective mass $m_{\text{eff}}(\tau)$ with its antiparticle counterpart $-m_{\text{eff}}(1 - \tau)$. The Δm_{eff} correction becomes negligibly small only if $\tau < \frac{1}{2}$ or $\tau > N - \frac{1}{2}$ [cf Eq. (18)]. The lower curve of Fig. 3 corresponds to the large- M case. The medium curve of the same figure shows the $m_{\text{eff}}(\tau)$ dependence for M far from both extremes; it shares to some extent the features of the two limiting cases.

Finally, we consider the heavy-fermion case ($\mu \gg M$). Here, as we have discussed earlier, G_N is dominated by the vicinity of the Gaussian peak. It follows that

$$\Delta m_{\text{eff}} = -8kM. \quad (28)$$

Again, this is the only case where the copying yields a relatively small correction. An example of this situation is given by the $\mu = 2 \times 10^3$ curve of Fig. 4. The second, $\mu = 500$ curve of this figure shows partial suppression of the oscillations by a smaller bare mass.

IV. DISCUSSION

We have studied in detail the effect of field configuration copying on both fermion and fermion-antifermion composite state correlation functions in a simple quantum-mechanical model. One could hope that the configuration repetition would allow a reliable extraction of low-lying excitation energies in a wider range of values of the time separation. This, however, does not turn out to be the case, unless the interaction can be neglected compared to the fermion bare mass term. Instead, we obtain a variety of possibilities for the effective mass behavior, depending on the temperature and the bare mass

value. For light fermions at high temperature the effective mass correction is constant within a copy but has a discontinuity on a copy boundary. On the other hand, the correlation functions at low temperatures develop an oscillatory behavior. The fermion correlator in the first copy remains unaffected by the oscillations. In the meson correlator, however, the oscillations penetrate even into the first copy for $\tau > \frac{1}{2}$. Altogether, we find no region in the parameter space where the configuration repetition is useful for spectrum measurements. There is at best a single copy where the one-copy results are approximately reproduced.

A natural question arises as to what extent the results presented here should be expected in other models. In quantum mechanics the effective mass oscillations are likely to follow from the background-field configuration repetition. Indeed, a propagator $\Gamma(\tau)$ in the periodic background potential $V(\tau)$ should obey the Euclidean equation of motion

$$\left(\frac{d}{d\tau} + \mu + V(\tau)\right)\Gamma(\tau) = \delta(\tau). \quad (29)$$

Obviously, the effective mass in a fixed background configuration includes an oscillating term $V(\tau)$. This property of the propagator will survive averaging over configurations as it does in the example given here, unless some miraculous cancellations occur. Recent QCD calculations on replicated lattices seem to fit into a similar scenario. In particular, one of them finds an oscillatory

behavior of the pion effective mass beginning shortly after $\tau = 0.5$. If the origin of these oscillations is common to QCD and our simple model, so must be the conclusion: replicating lattices does not increase the amount of useful spectroscopic information that can be extracted from correlation functions. Therefore this technique is of doubtful value for hadron spectroscopy calculations.

ACKNOWLEDGMENTS

I am indebted to S. Gottlieb, G. P. Lepage, R. L. Sugar and D. Toussaint for stimulating discussions. I also wish to thank E. G. Klepfish for useful remarks. This work was supported by the U.S. Department of Energy.

APPENDIX:

In this appendix we describe the method used to calculate the F_N and G_N integrals numerically. For the sake of brevity we concentrate on the continuum limit, in which

$$F_N(\tau) = \int du \frac{1 + e^{2\sqrt{M}u}}{1 + e^{2N\sqrt{M}u}} e^{(N-\tau)2\sqrt{M}u - (u-\mu/2\sqrt{M})^2}. \quad (A1)$$

Expanding the denominator of the integrand in Eq. (A1) in powers of $\exp(2N\sqrt{M}u)$ for $u < 0$ or its inverse for $u > 0$ and integrating over u we find

$$F_N(\tau) = e^{-\mu^2/4M} \sum_{k=0}^{\infty} \sum_{q=0}^1 (-1)^k [e^{P_q^+(k)^2} \operatorname{erfc}(P_q^+(k)) + e^{P_q^-(k+1)^2} \operatorname{erfc}(P_q^-(k+1))], \quad (A2)$$

where

$$P_q^{\pm}(k) \equiv \sqrt{M}(kN \pm (\tau - q)) - \frac{\mu}{2\sqrt{M}} \quad (A3)$$

and erfc denotes the complementary error function. This alternating series is convergent for all values of τ because $\exp(-x^2)\operatorname{erfc}(x) \propto x^{-1}$ for large positive x . Obviously, the convergence slows down for small M . We use Cesaro's summation by arithmetic means to improve the convergence in our numerical computation of Eq. (A2). Truncating the series after the eighth term yields a 3%

error in Δm_{eff} relative to M in a wide range of all the involved parameters for $N = 1$ (where the exact value of Δm_{eff} is 0), 2, or 4.

A similar method is applied to calculate $G_N(\tau)$ of Eq. (25). Here, however, a straightforward expansion of the denominator in powers of $\exp(\pm 2N\sqrt{M}u)$ does not lead to convergent series expansion. The latter is obtained by first integrating by parts to replace $\cosh^{-2}(N\sqrt{M}u)$ with $\tanh(N\sqrt{M}u)$. The resulting expansion reads

$$G_N(\tau) = \frac{1}{N\sqrt{M}} e^{-\mu^2/4M} \left(4 + \sum_{k=1}^{\infty} (-1)^k \sum_{q=-1}^1 (2 - q^2) \{ 2 - \sqrt{\pi M} k N [e^{Q_q^+(k)^2} \operatorname{erfc}(Q_q^+(k)) + e^{Q_q^-(k)^2} \operatorname{erfc}(Q_q^-(k))] \} \right), \quad (A4)$$

where

$$Q_q^{\pm}(k) \equiv \sqrt{M} \left[(k \mp 1)N \pm \left(2\tau - q - \frac{\mu}{2M} \right) \right]. \quad (A5)$$

As in the F_N case, individual terms in this alternating series decrease as k^{-1} for large k . However, the conver-

gence is much slower this time, especially for small values of M . We overcome this difficulty by using the powerful Euler's summation method. With the eighth term included, this gives the result as accurate as in the F_N case.

- ¹E. Marinari, G. Parisi, and C. Rebbi, Phys. Rev. Lett. **47**, 1795 (1981).
- ²K.C. Bowler, G.S. Pawley, D.J. Wallace, E. Marinari, and F. Rapuano, Nucl. Phys. **B220**, 137 (1982).
- ³P. Hasenfratz and I. Montvay, Phys. Rev. Lett. **50**, 309 (1983).
- ⁴B.A. Thacker and G. Peter Lepage, Phys. Rev. D **43**, 196 (1991).
- ⁵Khalil M. Bitar *et al.*, Phys. Rev. Lett. **65**, 2106 (1990); Phys. Rev. D **42**, 3794 (1990).

- ⁶A. Krasnitz, Phys. Rev. D **42**, 1301 (1990). The correlation functions defined in that work and in the present one are related by the transformation $\tau \rightarrow 1 - \tau$, so that the first copy in the former corresponds to the last copy in the latter and vice versa. Clearly, this difference in conventions has no effect on the physics.
- ⁷Robert E. Pugh, Phys. Rev. D **33**, 1027 (1986).
- ⁸L.D. Faddeev, in *Methods in Field Theory*, proceedings of the Les Houches Summer School, Les Houches, France, 1975, edited by R. Balian and J. Zinn-Justin, Les Houches Summer School Proceedings Vol. 28 (North-Holland, Amsterdam, 1976).